

The mineralogical record of $f\text{O}_2$ variation and alteration in Northwest Africa 8159. Evidence for interaction between a mantle derived martian basalt and a crustal component(s). Charles, K. Shearer¹, Paul V. Burger¹, Aaron S. Bell¹, Francis M. McCubbin¹, Carl Agee¹, Justin I. Simon² and James J. Papike¹. ¹Institute of Meteoritics, Department of Earth and Planetary Science, University of New Mexico, Albuquerque, New Mexico 87131, ²NASA Johnson Space Center, Houston, TX 77058.

Introduction: A prominent geochemical feature of basaltic magmatism on Mars is the large range in initial Sr isotopic ratios ($\sim 0.702 - 0.724$) and initial ϵ^{Nd} values (~ -10 to $>+50$). Within this range, the shergottites fall into three discrete subgroups. These subgroups have distinct bulk rock REE patterns, mineral chemistries (i.e. phosphate REE patterns, Ni, Co, V in olivine), oxygen fugacity of crystallization, and stable isotopes, such as O. In contrast, nakhlites and chassignites have depleted ϵ^{Nd} values ($\geq +15$), have REE patterns that are light REE enriched, and appear to have crystallized near the FMQ buffer (e.g. [5] and references within).

The characteristics of these various martian basalts have been linked to different reservoirs in the martian crust and mantle, and their interactions during the petrogenesis of these magmas [e.g. 1-5]. These observations pose interesting interpretive challenges to our understanding of the conditions of the martian mantle (e.g. $f\text{O}_2$) and the interaction of mantle derived magmas with the martian crust and surface.

Martian meteorite NWA 8159 is a unique fine-grained augite basalt derived from a highly depleted mantle source as reflected in its initial ϵ^{Nd} value, contains a pronounced light REE depleted pattern, and crystallized presumably under very oxidizing conditions [6,7]. Although considerably older than both shergottites and nakhlites, it has been petrogenetically linked to both styles of martian magmatism. These unique characteristics of NWA 8159 may provide an additional perspective for deciphering the petrogenesis of martian basalts and the nature of the crust of Mars.

Analytical Approach: Thin sections of NWA 8159 were initially examined and documented using backscattered electron imaging (BSE) on the JEOL JXA-8200 Superprobe electron microprobe (EMP) in the Institute of Meteoritics at the University of New Mexico (UNM). Wave-length dispersive X-ray maps were collected for Cr, Ca, Mn, P and Ti, while energy dispersive (EDS) maps were collected for Mg and Fe. Maps were collected using a 15 kV accelerating voltage, a 500 nA beam current and a dwell time of 800 ms/pixel. Quantitative point analyses were conducted of various silicates and oxide phases using the EMP. The point analyses employed an accelerating voltage of 15 kV, a beam current of 20 nA, and a spot size varying from 1-3 μm .

An FEI Quanta 3D Field Emission Gun FIB/SEM/EDS was used to image sample texture and

chemistry at the nanoscale, focus on a specific nanoscale region, and cut and thin micro-scale wide, nano-scale thick sections for transmission electron microscope (TEM) analysis. The locations of the FIB cuts were primarily within cores of the olivine. A JEOL 2010 TEM with Oxford INCA system ultrathin window EDS (energy dispersive spectroscopy) detector for nanoscale chemical analysis of light to heavy elements was used for sample mapping of chemistry and selected area diffraction for phase analysis. A JEOL 2010F FASTEM field emission gun capable of scanning transmission electron microscopy (STEM/TEM) with point to point resolution of 0.194 nm and minimum probe size of 0.14 nm was used for diffraction contrast and energy filtered TEM imaging. It is equipped with a Gatan GIF image filtering system for energy filtered TEM and electron energy loss spectroscopy (EELS), and an Oxford INCA system with ultrathin window EDS detector for nanoscale chemical analysis of light to heavy elements.

Chromium K-edge XANES data were acquired with the X-ray microprobe of GSECARS beamline 13-ID-E at the Advanced Photon Source (APS), Argonne National Laboratory, Illinois. The X-ray source at APS beamline 13-ID-E was a 72-pole, 33 mm period undulator. The beam was focused to a final spot size of $\sim 5\mu\text{m}$ by $5\mu\text{m}$ with dynamically configured Kirkpatrick-Baez focusing mirrors. All spectra were acquired in fluorescence mode utilizing a cryogenically cooled Si(311) monochromator and a silicon-drift solid state detector offset at a 45° angle from the sample. Spectra were acquired in three distinct crystallographic orientations and merged in order to mitigate the effects of crystalline anisotropy on the intensity of the peak associated with the 1s-4s transition [8,9].

Results: BSE imagery of olivine (50-200 μm) and adjacent phases illustrate olivine cores exhibit alteration and that adjacent orthopyroxene (opx) spatially associated with olivine rims are intergrown with magnetite (mag) (Fig. 1). Similar textures have been identified in nakhlites [5] and terrestrial basalts and gabbros [e.g. 10-13]. X-ray maps (Fig. 1) and point analyses illustrate that the “olivine” cores have higher Mg# ($\text{Mg}/(\text{Mg}+\text{Fe})$) than rims and that they are enriched in P (up to 1.4 wt%) and Al_2O_3 . TEM imaging and analyses of the “olivine” core indicates that it is an intergrowth of olivine plus multiple non-magmatic phases. The alteration appears to be

unrelated to terrestrial carbonate that occurs in veins that cross-cut martian silicates. The valence state of Cr (Cr , Cr^{3+}) in unaltered and modified olivine indicate all Cr is in the trivalent valence state. Ni concentrations in the olivine are less than 150 ppm. The opx associated with the olivine rims has a very low Wo content (Wo_{2-1}) and exhibits zoning in Mg# from 0.29-0.60. The opx with the higher Mg# are generally intergrown with the mag. The mag in the intergrowths is essentially end-member mag with very small amounts of TiO_2 or Cr_2O_3 . Based on pyroxene stoichiometry, the $\text{Fe}^{3+}/(\text{Fe}^{3+}+\text{Fe}^{2+})$ of the opx is less than 2%. The $\text{Fe}^{3+}/(\text{Fe}^{3+}+\text{Fe}^{2+})$ in the clinopyroxene ($\text{Wo}_{40}\text{En}_{35}\text{Fs}_{25}$ to $\text{Wo}_{22}\text{En}_{18}\text{Fs}_{60}$) is only slightly higher and more variable ($>3\%$).

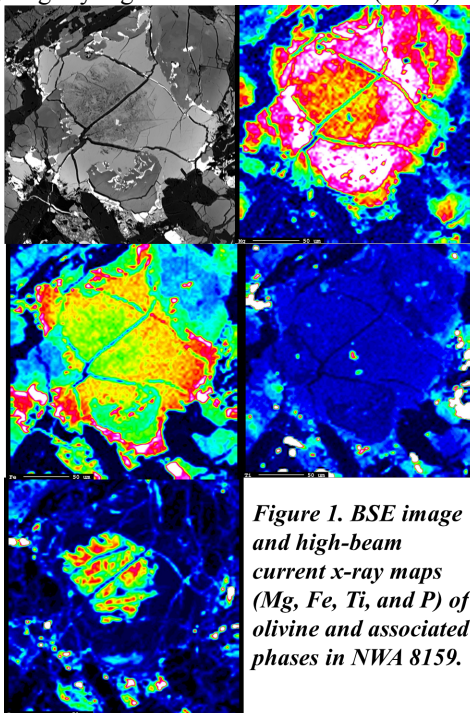


Figure 1. BSE image and high-beam current x-ray maps (Mg, Fe, Ti, and P) of olivine and associated phases in NWA 8159.

Discussion: Several interesting observations potentially provide insight into the petrogenesis of NWA 8159. The mag-opx intergrowths such as those associated with the small olivine grains in NWA 8159 have been attributed to both magmatic [e.g. 5,10,12] and very late-stage magmatic to subsolidus [e.g. 12,13] processes and are produced at particular $f\text{O}_2$ conditions. Presnall [12] demonstrated that the magmatic processes producing this texture reflect a reaction occurring at the olivine-pyroxene-spinel peritectic ($\text{olivine} + \text{peritectic liquid} \leftrightarrow \text{spinel} + \text{opx}$) in the MgO -iron oxide- SiO_2 system (1326°C at FMQ+1). An interesting point from the experiments of [12] is that only at $f\text{O}_2$ conditions several log units above FMQ does the Fe-Ti spinel composition even approach end-member mag compositions. Most recently, results from [14,15] were interpreted as indicating that for Fe-rich martian magmas end-

member mag was produced either at conditions much more oxidizing than FMQ or at subsolidus conditions. Morse [13] suggested that the “oxysymplectites” of mag + opx were produced by the interaction of olivine with either a late-stage Fe-rich residual liquid with excess oxygen or an oxygen-rich vapor phase released near the end of crystallization. Yoder and Tilley [12] provided examples of potential subsolidus reactions. One potential reaction relevant to NWA 8159 is $3 \text{ ol} + \frac{1}{2}\text{O}_2 \leftrightarrow 3 \text{ opx} + \text{mag}$ [5,12]. Using mineral compositions from NWA 8159 this reaction occurs at $f\text{O}_2$ conditions of FMQ-1.94 (at 700°C) to FMQ-0.979 (at 1000°C). These calculations suggest that end-member mag is produced at somewhat more reducing conditions than implied for a magmatic origin. The measured valance state for Cr and calculated for Fe are consistent with these $f\text{O}_2$ conditions for Fe-rich martian magmas [6,15].

Subsolidus alteration is reflected in the preferential modification of the P-rich cores of the olivine. This correlation may imply that the P enrichment in the olivine cores is magmatic and that the alteration is martian in origin. Other martian basalts have olivines that exhibit substantial P zoning, although P concentrations in NWA 8159 are considerably higher [4]. The link between this alteration and the opx + mag intergrowths is unknown. Further examination of the alteration mineralogy of the olivine cores continues using TEM.

In summary, NWA 8159 appears to have many geochemical and mineralogical characteristics that are generally similar to nakhlites. These characteristics reflect some near-solidus to subsolidus processes. These include oxidation of olivine and preferential alteration of phosphorous-rich cores of olivine. These processes may reflect the addition of a crustal signature to the nakhlites which is also reflected in the Cl-isotopic characteristics of these lithologies [16]. There still are distinctive differences, however, such as its initial ϵ^{Nd} value ($\sim +45$) [7] that suggest it may have some affinity to the petrogenesis of both recognized styles of martian magmatism.

References: [1] Herd et al. (2002) *GCA* 66, 2025-2036. [2] Wadhwa (2001) *Science* 291, 1527-1530. [3] Synes et al. (2008) *GCA* 72, 1696-1710. [4] Shearer et al. (2013) *GCA* 77, 17-38 [5] Treiman and Irving (2008) *MAPS* 43, 829-854. [6] Agee et al. (2014) 77th Met Soc meeting Abstr. 5397. [7] Simon et al. (2014) 77th Met Soc meeting Abstr. 5363. [8] Bell et al. (2014) *Am. Min.* 99, 1404-1412. [9] Berry et al. (2006) *Am. Min.* 91, 1901-1908 [10] Kuno (1950) *GSA Bull.* 61, 957-1020. [11] Presnall (1966) *AJS* 264, 753-809. [12] Yoder and Tilley (1962) *Jour. Pet.* 3, 342-532. [13] Morse (1969) *GSA Mem* 112. [14] Righter et al. (2013) *Am. Min.* 98, 616-628. [15] Papike et al. (2015) *Am. Min.* 100, in press. [16] Shearer et al. (2014) workshop on volatiles in the martian interior. Abstr. #1021.